

# **Evaluating Feasibility of Incorporating Fuel Cell Drive Trains into Existing Haul Trucks**

Ayorinde Akinrinlola<sup>1</sup> · Kwame Awuah-Offei<sup>1</sup> · Abdullah Al Moinee<sup>1</sup>

Received: 24 June 2025 / Accepted: 4 September 2025 © The Author(s) 2025

#### **Abstract**

Hydrogen, as a fuel source in material handling, has become a viable option for achieving carbon reduction targets. The objective of this work was to apply vehicle drive train and energy simulation in MATLAB/Simulink to guide a discussion of the challenges and opportunities of incorporating hydrogen fuel cell drive trains into the current form factors of mine haul trucks. We built and validated a model based on the Komatsu 830-E truck and used it to estimate the hydrogen requirements for typical short-haul, medium-haul, and long-haul cycles; in the short-haul case (cycle time = 852 s) the truck consumed 23.6 L of diesel compared to 17,729 L of hydrogen at standard temperature and pressure (STP), and in the medium-haul case it consumed 29.0 L of diesel compared to 24,081 L of hydrogen at STP. We also estimated the size of the required fuel cell stack based on power, voltage, and current demands. The results show that the truck requires 75.98–110.16 L and 37.99–55.08 L of hydrogen at 350 and 700 bars, respectively, compared to 23.60–82.92 L of diesel. To retrofit a diesel haul truck with a hydrogen fuel cell drive train with the same driving range, the most likely pressure for hydrogen storage must be 700 bars. Even at 700 bars, the current diesel trucks do not have adequate space to install the hydrogen storage, fuel cell stack, and other components of the fuel cell drive train to allow for retrofitting them as hydrogen fuel cell trucks. Thus, the mining industry's adoption of hydrogen fuel cell trucks will likely require a more extensive redesign with significant investment from original equipment manufacturers. Additionally, mining companies that adopt hydrogen fuel cell trucks must address safety and security risks and invest in hydrogen storage and transportation infrastructure.

Keywords Mine haulage · Haul trucks · Fuel cell · Drive train modeling · Renewable energy

# 1 Introduction

Decarbonization has become one of the top issues for the mining sector in recent years. For example, Ernst & Young's annual survey of business risks and opportunities has listed decarbonization among the top five risks and opportunities since 2020. The mining industry is responsible for about 4–7% of global greenhouse gas emissions [1]. While the greenhouse gas emissions of individual mined products vary, the life-cycle emissions of some mined products are high, particularly for certain metals required for green energy solutions to mitigate climate change. A significant portion of mining-related greenhouse gas (GHG) emissions comes

from methane emissions in coal mines, while the remainder stems from GHG emissions related to mining operations, including material handling and energy usage in mines. Several mining companies, including members of the International Council on Mining and Metals (ICMM), have committed to decarbonization targets in response to investor and social expectations [2]. As a result, the mining sector has been exploring ways to reduce carbon emissions through electrification and other initiatives. Material handling is a significant source of greenhouse gases due to its energy intensity [3]. Truck haulage, a popular method of material handling because of its flexibility, is a major contributor to greenhouse gas emissions due to the mining industry's reliance on diesel fuel to power haul trucks. Emissions from mining vehicles amount to over 68 million tonnes of CO<sub>2</sub>-eq each year, accounting for 30-80% of the total GHG emissions from mining operations [4]. Consequently, the mining sector has dedicated considerable effort to improving the

Published online: 27 October 2025



Kwame Awuah-Offei kwamea@mst.edu

Department of Mining & Explosives Engineering, O'Keefe Center for Critical Minerals, Missouri University of Science & Technology, MO, Rolla 65401, USA

energy efficiency of haul trucks and finding ways to integrate clean energy sources into truck haulage.

Electric trucks, such as Epiroc's Minetruck MT42 Battery Truck, a 42-ton articulated underground vehicle, powered by lithium-ion batteries [5], are the most common approach to electrifying the mining truck haulage fleet. The use of electric trucks can enable mining operations to take advantage of renewable energy sources to reduce their greenhouse gas emissions. However, the disadvantages of battery-electric trucks include low energy density, high upfront costs, extended charging times (mining applications often use battery swapping, to overcome this limitation), short lifespan, and safety concerns in the event of battery failure [6]. Trolley-assist mine truck haulage [7] also provides opportunities to leverage renewable energy capacity from the grid, thereby minimizing reliance on diesel. Trolley-assist offers some of the same advantages as battery-electric trucks without relying on battery storage. However, it also comes with a significant upfront cost to install trolley lines and still requires diesel power for portions of the duty cycle not covered by trolley-assist (trolley lines are often installed only on the main haulage ramps).

Despite the current best available technology, the benefits of electric-powered haulage are limited by the fossil fuel content in the electricity mix of the jurisdiction in which the mine operates (or how much renewable "electrons" the mine can purchase from utilities). The current energy mix for the grids that mines draw from means mines contribute to GHG emissions to the same extent as the fossil fuel content of the electricity grid. Coal, oil, and natural gas continue to provide significant portions of electricity generation in major mining countries, including China, India, the USA, and European Union [8]. Additionally, in remote mines that are not connected to the electric grid, electrification alone does not lead to decarbonization unless coupled with renewable energy generation on-site. While renewable installations at mines have increased from 42 MW annually in 2008 to 3397 MW in 2019 [9], they are still not the dominant energy source utilized for mining operations. This limitation has motivated interest in hydrogen fuel cell trucks, which can generate onboard power independent of the grid while still offering zero tailpipe emissions.

As a result, some mining companies and original equipment manufacturers (OEMs) have been exploring hydrogen fuel cell powered trucks due to their ability to generate onboard clean energy. Fuel cells, when deployed with batteries as hybrid electric vehicles, improve energy density and driving range, and reduce charging times [10] [11]. Examples of such technology include Toyota's Mirai passenger vehicle [12] and Hyundai's Xcient highway truck [13]. The Toyota Mirai has a driving range of 402 miles, competing with the average range of conventional vehicles (300–400 miles) [12]. This concept can serve as a template

for implementing well-performing electric mining trucks. In fact, Anglo American, in collaboration with Komatsu and First Mode, is piloting a hydrogen fuel cell hybrid electric truck at their Mogalakwena Mine in South Africa [14]. Unlike batteries, hydrogen fuel cells do not necessarily require frequent recharging because they generate energy via a chemical reaction between hydrogen and oxygen. This process produces an electric current that can drive electric motors while emitting only water and heat as waste. Thus, hydrogen fuel cells can power heavier-duty trucks, either as a hybrid with batteries or standalone, with a more extended operation duration than lithium-ion battery packs due to their energy density and the ability to refuel in minutes, whereas recharging the battery needs hours [10].

The quick deployment of hydrogen fuel cells in mining trucks will likely involve using the same truck design and replacing the diesel drive-train components with batteries and fuel cell stacks. This poses challenges in terms of efficiently using the truck's "real estate" to power the trucks and achieve similar productivity and driving range. These are pertinent and timely questions that require rigorous analysis to inform decarbonization strategies for mine haulage. Unfortunately, despite growing interest, there is a dearth of published research evaluating the feasibility of fuel cell truck haulage, although mining firms and OEMs have undoubtedly conducted these analyses in proprietary forms. Therefore, the objective of this work is to apply vehicle drive train and energy simulation in MATLAB/Simulink to elucidate the challenges and opportunities of incorporating hydrogen fuel cell technology into the current form factors of mine haul trucks. We achieved this objective by building a drive train model of a fuel cell truck in MATLAB/ Simulink. The novelty of this work lies in its use of drive train simulation (validated with field data) to explore the feasibility and challenges of fuel cell mining truck haulage. This evaluation is crucial because government policy and private funding decisions will rely on such analyses, and it is in the public interest to have these analyses published in the open literature. The work is also novel because, unlike others published for smaller vehicles, it uses realistic mining haul cycles and associated duty cycles to estimate energy demands and hydrogen consumption.

# 2 Fuel-Cell Haul Truck Drive-Train Modeling and Simulation

Converting diesel-electric haul trucks to hydrogen fuel cell electric trucks presents a promising pathway for reducing GHG emissions in the mining sector while maintaining operational performance. This work assesses the feasibility of converting a diesel-powered haul truck into a hydrogen fuel cell truck. Since diesel-powered trucks are well



established within the mining industry, the goal of this work was to use a hydrogen fuel cell truck model to evaluate the challenges of incorporating a hydrogen fuel cell truck into the existing design of the diesel-powered truck. Specifically, the modeling approach in this study is built on existing truck specifications to assess whether a fuel cell system can match or exceed current performance standards while conforming to physical and operational constraints. This is important because converting the fleet of existing trucks is the most likely way for the broad adoption of fuel cell technology in mining. The main advantage of using the architecture of an existing mining haul truck is that it allows engineers to directly compare performance characteristics and infrastructure requirements between the two systems. This approach facilitates a realistic feasibility analysis, as it leverages known parameters such as weight, power demand, energy losses, and operational drive cycles. For example, in this study, the authors used the Komatsu 830E-5 truck specifications to build the model and experiment based on drive cycle data obtained from the truck during a mine operation. The truck's specification and drive cycle serve as a reference for the model and allow one to obtain power demand and corresponding hydrogen fuel consumption during a particular drive cycle (this model should work for any truck specification so long as the analyst has the data to specify the truck). The fuel consumption estimate enables us to predict the required size of the onboard hydrogen storage. Furthermore, it allows us to see if the storage sizes fit the current geometry or "real estate" of the existing mining haul trucks without significant changes to the truck's structure and design. Figures 1 and 2 present an overview of the drive system of the diesel-electric drive truck and the proposed fuel cell electric drive truck, illustrating the fundamental difference in drive system architecture between the diesel-electric and proposed hydrogen fuel cell electric trucks.

Figure 1 shows the conventional diesel-electric configuration, where a diesel internal combustion (IC) engine drives an alternator to generate AC power, which is then conditioned through a transformer and rectifier, inverted, and delivered to the electric drive motor connected to the wheels.

In contrast, the hydrogen fuel cell electric system, presented in Fig. 2, replaces the diesel engine and alternator with a fuel cell stack supported by a battery system. The hydrogen fuel cell generates electricity directly from hydrogen stored onboard, and this power, along with supplemental power from the battery, is processed through an inverter to drive the motor and, ultimately, the wheels.

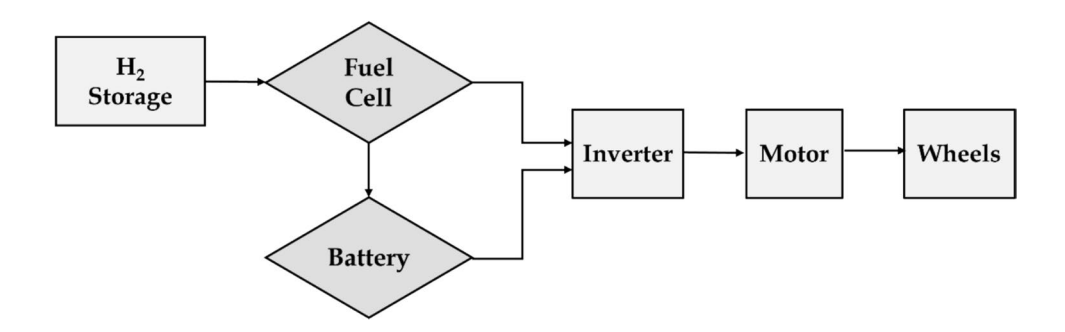
This section of the paper presents the fuel cell truck modeling and verification process, as well as simulation experiments conducted to estimate the onboard hydrogen tank size requirements. The model consists of three primary subsystems: the driver sub-model (which includes the drive cycle and control strategy), the powertrain sub-model (fuel cell, battery, inverter, and motor), and the vehicle dynamics sub-model (mass, aerodynamic drag, rolling resistance, and road gradient).

We validated the model using a base-case experiment that replicates the operational cycle of the reference truck. The simulation outputs include total power demand, fuel cell output, battery usage, and cumulative hydrogen consumption. From these data, we estimate the total hydrogen required to complete the drive cycle and translate this to the volume and mass of hydrogen storage needed onboard. Additionally, the simulation results inform the sizing of the fuel cell stack to ensure that the power output is sufficient to meet peak and average demands during haul operations. These findings enable a comparative analysis of spatial requirements and integration feasibility, evaluating whether hydrogen storage systems can fit within the geometrical constraints of existing truck designs without significant structural modifications.



Fig. 1 Overview of diesel-electric drive truck

Fig. 2 Overview of the proposed fuel cell electric truck





# 2.1 Modeling

This section presents the essential aspects of the simulation model and shows key specifications of the Komatsu 830E-5 diesel-powered haul truck (Table 1), which is used to select the basic requirements such as the chassis, torque, and power requirement of the simulated haul truck.

The authors developed the models in the MATLAB/ Simulink environment. The input data that drives the model is the drive cycle data (velocity–time, vehicle weight, and inclination data) obtained from Komatsu 830E diesel-electric mine haul trucks in an actual mining operation. A driver subsystem model receives the velocity–time data and uses it to predict the required acceleration or braking to achieve the velocity at each time step in the data. The output of the driver sub-model is fed to the powertrain sub-model, which predicts the required power, torque, and force from the power supply and wheel, respectively. The truck model was designed using basic concepts of vehicle motion.

Figure 3 shows an overview of the model with the main components (each component is a subsystem explained further in the subsequent sections).

# 2.1.1 Driver Model

The driver model takes in the truck velocity-time data as the desired speed and the feedback velocity of the simulated truck as input. The sub-model uses a feedback mechanism

**Table 1** Key specifications of the Komatsu 830E-5 truck [15]

Attributes	Value 1865 kW at 1800 rpm	
Gross power		
Tire diameter	3741 mm	
Nominal gross vehicle weight	408,875 kg	
Empty vehicle weight	182,051 kg	
Nominal rated payload	226,800 kg	
Calculated frontal area	$49.25 \text{ m}^2$	
Top speed	64.5 km/h	
ear ratio 32:1		
Fuel tank	4542 L	

to ensure that the actual velocity of the vehicle follows the desired velocity (velocity provided in the input data) by providing an acceleration and brake command as an output. The errors are derived when the desired velocity is compared to the simulated truck velocity. The driver sub-model uses a proportional-integral (PI) controller to minimize and control the error between the desired and feedback truck velocities. Equation (1) describes the control function of a PI feedback controller, where  $K_p$  is proportional gain,  $K_i$  is integral gain, e(t) is error signal distribution,  $T_i$  is integral time step, and e(t) is the initial value. Both the proportional and integral components have a gain that help manage different errors [16] [17].

$$u(t) = \underbrace{K_p e(t)}_{\text{Proportional component}} + \underbrace{\frac{K_i}{T_i} \int e(t)dt}_{\text{Integral component}} + c \tag{1}$$

# 3 Powertrain Model

Figure 4 shows an overview of the powertrain sub-model. The traction force and power request are the main outputs of the powertrain model. The model takes in the acceleration and brake command (values between -1 and 1) as inputs. The sub-model uses the maximum and minimum torque values of the motor and the acceleration and brake commands to derive the torque and acceleration at every time step. The sub-model obtains the torque as a product of the acceleration and brake commands and the maximum and minimum torque values, respectively. The requested torque is then the sum of the accelerating and braking torques.

The sub-model also estimates the power from the torque estimate and the motor angular velocity. The sub-model uses the velocity profile of the vehicle to obtain the angular velocity of the motor. First, the sub-model estimates the vehicle angular velocity from the tire radius, r, and the vehicle velocity. Then, the model estimates the motor angular velocity as a product of the vehicle angular velocity,  $\omega$ , and the gear ratio GR. Equation (2) shows

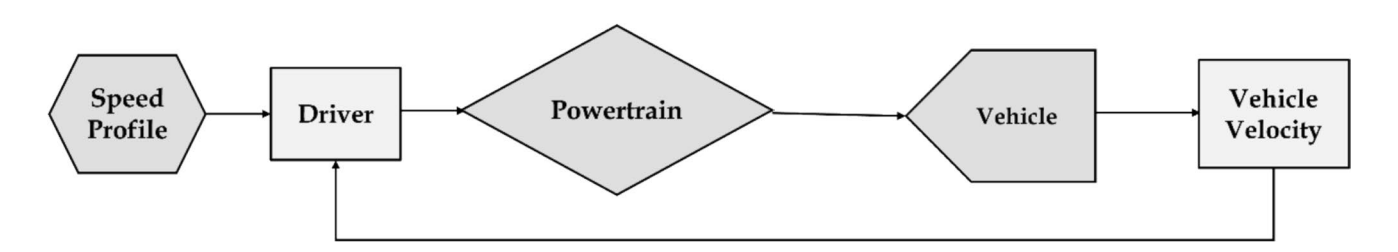


Fig. 3 Overview of the model at the system level



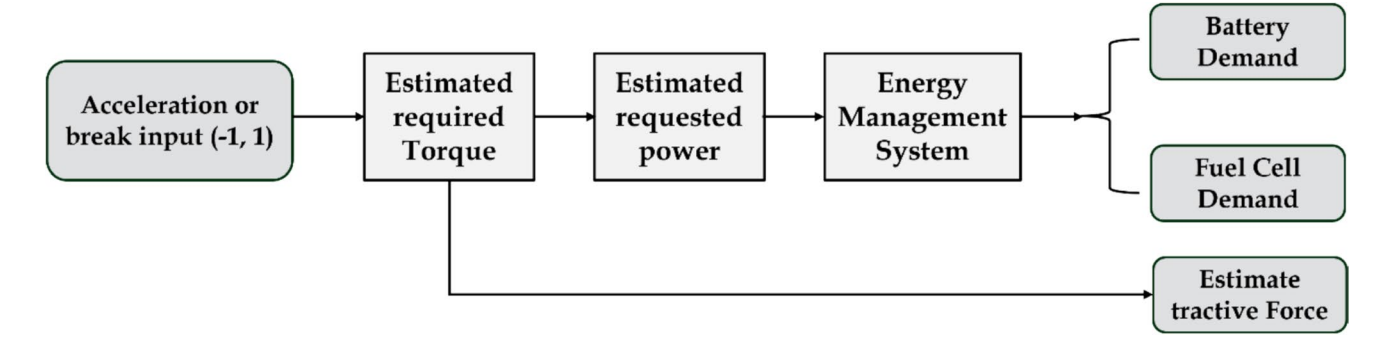


Fig. 4 Fuel cell signal variation parameters

the instantaneous power of the motor,  $P_m$ , as a function of the electric motor angular velocity,  $\omega_m$ , and the motor torque,  $\tau_m[18]$ .

$$P_m = \omega_m \tau_m = GR \times \omega \tag{2}$$

The sub-model also estimates the traction force from the requested torque. The traction force is adjusted to account for the braking effect by subtracting the product of the vehicle mass, brake command, gravity constant, and vehicle tire radius from the actual torque. These torque values multiply the tire radius to obtain the traction force passed to the vehicle model. The powertrain sub-model also includes an energy management system model that determines where the truck draws power from. The model in this study uses the fuel cell energy and battery sources that are available in Simulink. Just as the Hyundai Xcient fuel cell on-highway truck, the model assumes a fuel cell powered mining truck will have fuel cell stacks and batteries as energy sources. The Xcient fuel cell truck has a battery rated at 661V/73.2 kWh as support energy source in the vehicle, while the fuel cells can power up to 190 KW. The motor is rated at 350 kW capacity, and it has a hydrogen capacity of 32.09 kg<sup>-1</sup>. For the Toyota Mirai hydrogen fuel cell passenger car, the primary energy provider is the fuel cell while the battery helps with energy recovery during regenerative braking and assists the fuel cell sometimes during acceleration <sup>2</sup>. This study used these existing designs as guidelines during the modeling. However, the batteries are mainly used as an auxiliary energy source in fuel cell vehicles. For heavier vehicles with significant energy needs, adding more batteries detracts from the effective use of space, payload capacity, and fuel cell energy capacity. Therefore, the model tries to keep the energy needed from the batteries as close as possible to that of the Xcient fuel cell road truck. In this model, the power distribution determines the energy source based on the amount of power requested. When the battery exceeds 90% state-of-charge, regenerative braking is disabled to prevent overcharging, and excess braking energy is dissipated via friction brakes. Figure 5 shows the power source allocation algorithm in the model.

The power system runs on a 630-V nominal voltage, and the battery source is a battery of 100-kWh capacity, which helps with the regenerative braking and power requests of up to 200 kW. The fuel cell will provide energy for power requests of more than 200 kW.

The algorithm also ensures the system uses fuel cell power as a backup for when the battery is low. The model first determines whether the power request is positive or negative. Positive power request means energy should be provided to the truck, while negative power request indicates the truck generates energy that can be used to charge the battery. Therefore, all negative power values will go into the battery, provided that the battery's state of charge is less than 90%. The energy management system model tests for the magnitude of the power requests and the state of charge of the battery to determine which energy source will provide the power.

#### 3.1 Vehicle Model

Figure 6 illustrates the conceptual model of the primary forces acting on a vehicle during its motion on an inclined surface. These forces collectively determine the vehicle's dynamic behavior and are critical inputs to the vehicle modeling framework used in this study.

The tractive force, generated by the vehicle's power-train, acts in the direction of motion to propel the vehicle forward. Opposing this motion are several resistive forces: rolling resistance, caused by the deformation of tires and the road surface; grade resistance, resulting from the gravitational component acting along the slope defined by angle  $\theta$ ; aerodynamic drag, which increases with vehicle speed and opposes forward motion; and inertial force, representing the resistance to acceleration or deceleration due to the vehicle's mass. (Here, we distinguish between grade resistance and inertial force to align with the convention in the literature.)



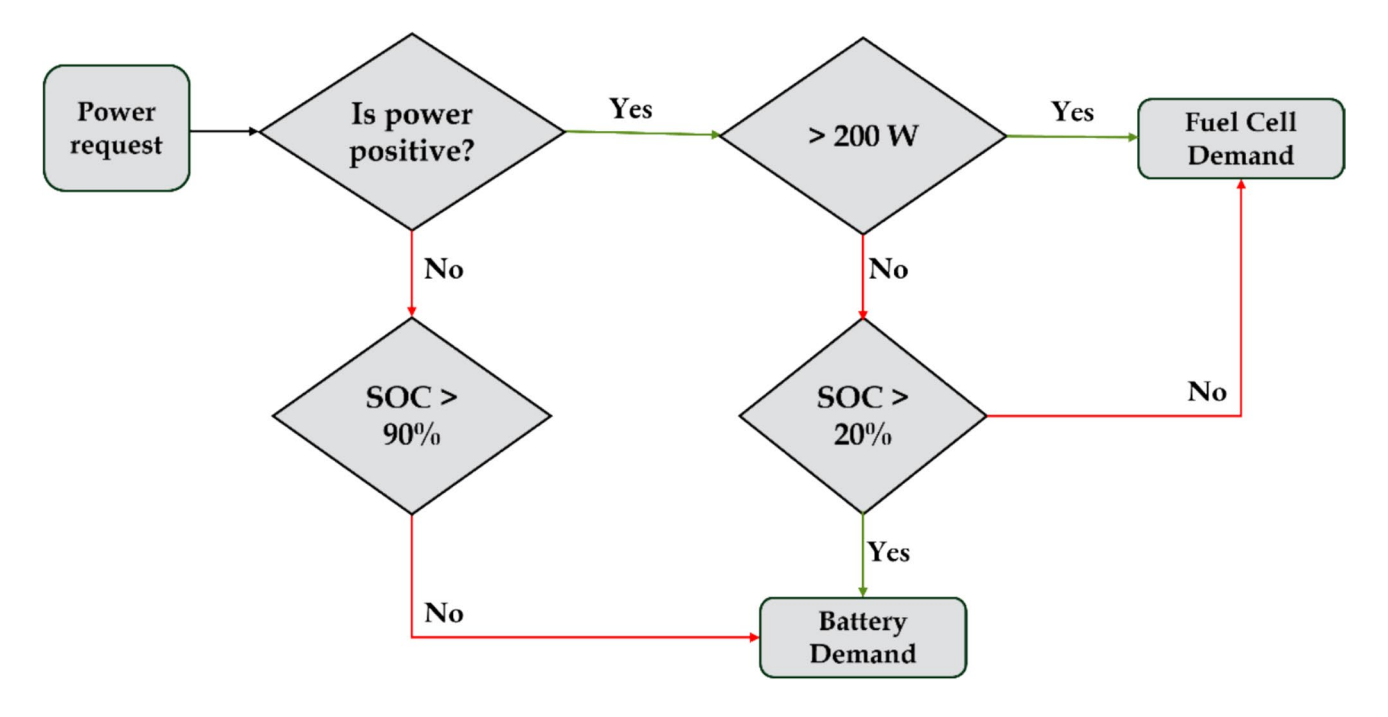


Fig. 5 Overview of the power distribution algorithm

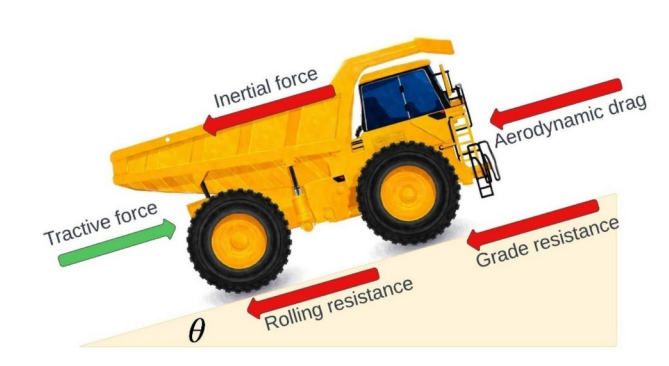


Fig. 6 Conceptual model of forces on vehicle

This force balance informs the development of the vehicle's longitudinal dynamics model, enabling accurate predictions of fuel consumption, velocity, and traction performance under varying terrain and load conditions.

The vehicle model estimates the propelling force from the resistances and the tractive force (provided by the powertrain model) by subtracting the resistances from the tractive force (Fig. 7).

The model estimates the acceleration from the mass of the vehicle, M, and the propelling force. The model estimates the vehicle velocity by integrating the acceleration. The model uses fundamental formulas to model and account for the aerodynamic drag, grade resistance, and rolling resistance. The aerodynamic drag is a resistive force in the opposing direction of the moving vehicle due to the air [19]. The airflow from high to low pressure caused by the moving

vehicle results in resistive forces opposite to the vehicle's direction. The model uses the generic aerodynamic drag equation (Eq. 3) that considers the drag coefficient, air density, velocity, and frontal area of the truck [20]. In the model in this work, this equation is implemented as a Simulink function that takes in the values of the vehicle velocity as a variable, and the constant values ( $\rho$ , A, and  $C_{\rm drag}$ ) and uses these to estimate the aerodynamic drag. V is the vehicle velocity,  $\rho$  is air density, A is the frontal area of the vehicle, and  $C_{\rm drag}$  is the drag coefficient.

Aerodynamic drag = 
$$0.5V^2 \rho A C_{\text{drag}}$$
 (3)

The grade resistance is the resistance to truck motion when it moves uphill on an inclined surface. The grade resistance depends on the vehicle's mass (M), the acceleration due to gravity (g), and inclination  $(\theta)$  (Eq. 4) [19]. The inclination changes with time during a typical mine drive cycle depending on the haul road profile, and the model in this work accounts for this by reading the inclinations from the input data.

Grade resistance = 
$$M \times g \times \sin(\theta)$$
 (4)

The rolling resistance is due to the constant contact between the tires of the vehicle and the surface of the road. A frictional force between the tires and the road acts as a form of resistance to the forward motion due to the traction force. As shown in Eq. 5, the rolling resistance depends on the mass of the vehicle, acceleration due to gravity, and inclination of the vehicle [19].



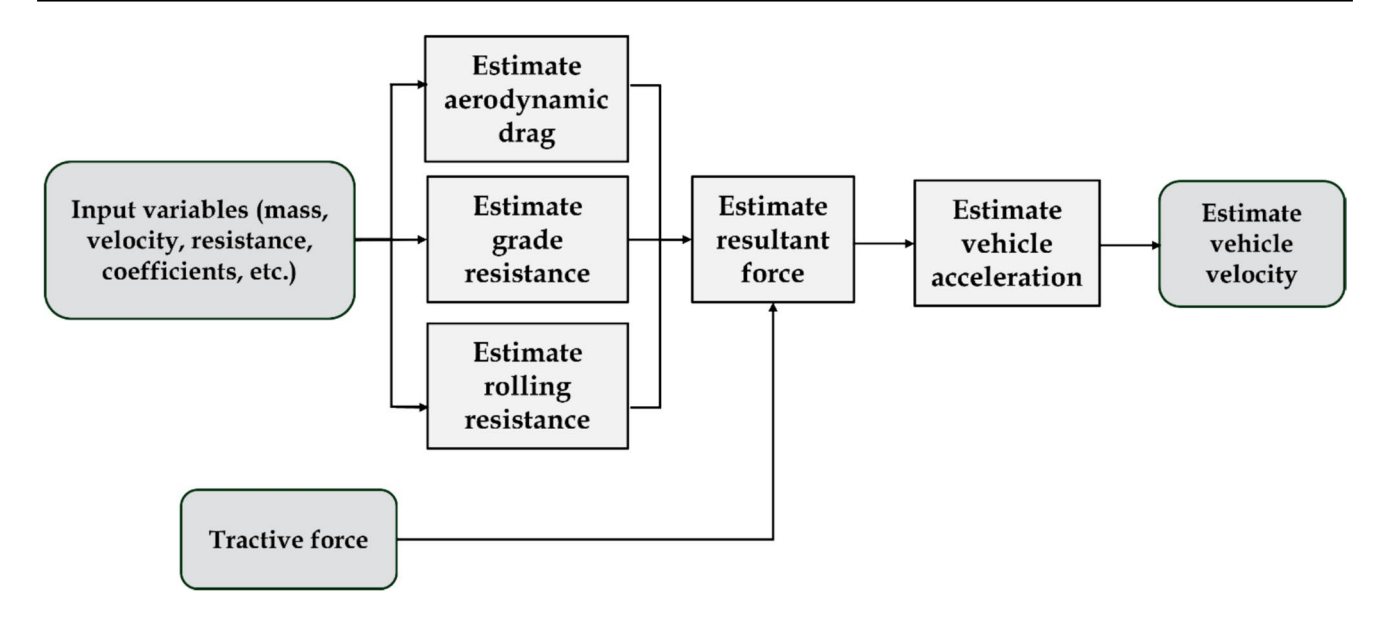


Fig. 7 Overview of vehicle model

Table 2 Vehicle parameters

Parameter	Value
Air density	1.225 kg/m <sup>3</sup>
Drag coefficient, $C_{\text{Drag}}$	0.65
Gravity, g	$9.81 \text{ m/s}^2$
Road angle, $\theta$	Varies
Rolling resistance coefficient, $C_{\text{rol}}$	0.03

Rolling resis 
$$\tan ce = M'g' \sin(q)$$
 (5)

#### 3.2 Model Verification

To verify the model, this work used data from a real mine running Komatsu 830E-5 trucks for verification. It was not possible to conduct validation because the authors did not have access to data from a hydrogen-powered truck. However, by verifying that the model behaved as intended, the authors believe that the model is useful for achieving the objectives of this work.

The main metric of verification was how closely the simulated vehicle velocity matched the desired (input) velocities. The model input for each simulation includes truck specifications, duty cycle (desired velocities, haul road profile, rolling resistance, etc.), and fuel cell specifications. Tables 2–4 contain the input data for the verification experiment. Table 2 contains the input data on the Komatsu 830E-5 truck, while Tables 3 and 4 contain fuel cell specifications.

In addition to these, the simulation requires duty cycle data. For this, the authors relied on data from a real mine

Table 3 Fuel cell nominal parameters

Parameter	Value	
Stack power	900 kW—Nominal 1500 kW—Maximal	
Fuel cell resistance	0.07224 Ohms	
Nerst voltage of one cell	1.1325	
Nominal utilization	Hydrogen = 99.94% Oxidant = 59.52%	
Nominal consumption	Fuel = $10,000 \text{ slpm}$ Air = $23,810 \text{ slpm}$	
Exchange current [i <sub>0</sub> ]	1.504 A	
Exchange coefficient [alpha]	-0.93237	

 Table 4 Fuel cell signal variation parameters

Parameter	Value
Fuel composition	99.95%
Oxidant composition	21%
Fuel flow rate at nominal hydrogen utilization	10,010 lpm—Nominal 20,020 lpm—Maximal
Air flow rate at nominal oxidant utilization	40,000 lpm—Nominal 80,000 lpm—Maximal
System temperature	273 K
Fuel pressure	1 bar
Air pressure	1 bar

(the authors are keeping the name of the mine confidential as per the non-disclosure agreement between Missouri S&T and Komatsu) that included 30 drive cycles over various haul routes and terrain. The authors selected a drive cycle



that was typical in the data set for verification. Figure 8 shows the grade (angle of inclination), weight, and velocity for the selected drive cycle. The duration of the drive cycle and, thus, the simulation is 1100 s (18.33 min).

Figure 8 illustrates the road grade (angle of inclination), total vehicle weight, and velocity profiles over a selected drive cycle lasting approximately 1100 s (18.33 min). The grade profile exhibits dynamic elevation changes, including uphill and downhill segments ranging from – 15° to + 15°, representative of realistic road conditions. The total weight shows a sharp increase midway through the cycle, simulating a loading event, followed by a gradual decrease toward the end, indicating unloading. The velocity profile captures typical drive cycle behavior with multiple stop-and-go phases, variations in acceleration, and extended idle periods, reflecting real-world operational dynamics used for the vehicle simulation Figs. 9–14 show the results of the verification experiments.

Figure 9 shows the simulated and input truck velocities. As shown by the figure, the simulated velocity matches the input velocities indicating the model's ability to replicate the drive cycle. This is the main metric for verification in this work. The truck duty cycles in the data used in this research

begin when the truck starts moving towards the shovel to get a load. The idle time shown in the cycle (t=420–637 s) is for when the truck is waiting at the shovel to get a load. Figure 10 shows the torque, angular velocity, and propelling force, while Fig. 11 shows requested power from the simulation. Based on the simulated power requests, the model predicts the fuel cell and battery power shown in Fig. 11.

The velocity output of the vehicle sub-model is directly related to the angular velocity at the wheel as a function of the gear ratio (Fig. 10b). These further builds confidence in the model as it implies the sub-models are consistent with the fundamental equations used to estimate truck parameters such as power, force and speed. Power is the product of angular velocity and torque (Eq. 2). A careful examination of the torque, angular velocity, and force (Fig. 10) together with the power (Fig. 11) shows the model is working as intended. An examination of Fig. 11 also shows that the battery and fuel cell power draws follow the power distribution system in the model (Fig. 5). Also, the entire power request (Fig. 11) is within the rated power of the 830E – 5 Komatsu truck, which has a gross operating power of 1865 kW.

Figure 12 shows the operating conditions of the fuel cell, which are aligned with the power specifications of the

Fig. 8 Input data about duty cycle: a haul road grade, b total weight, and c velocity

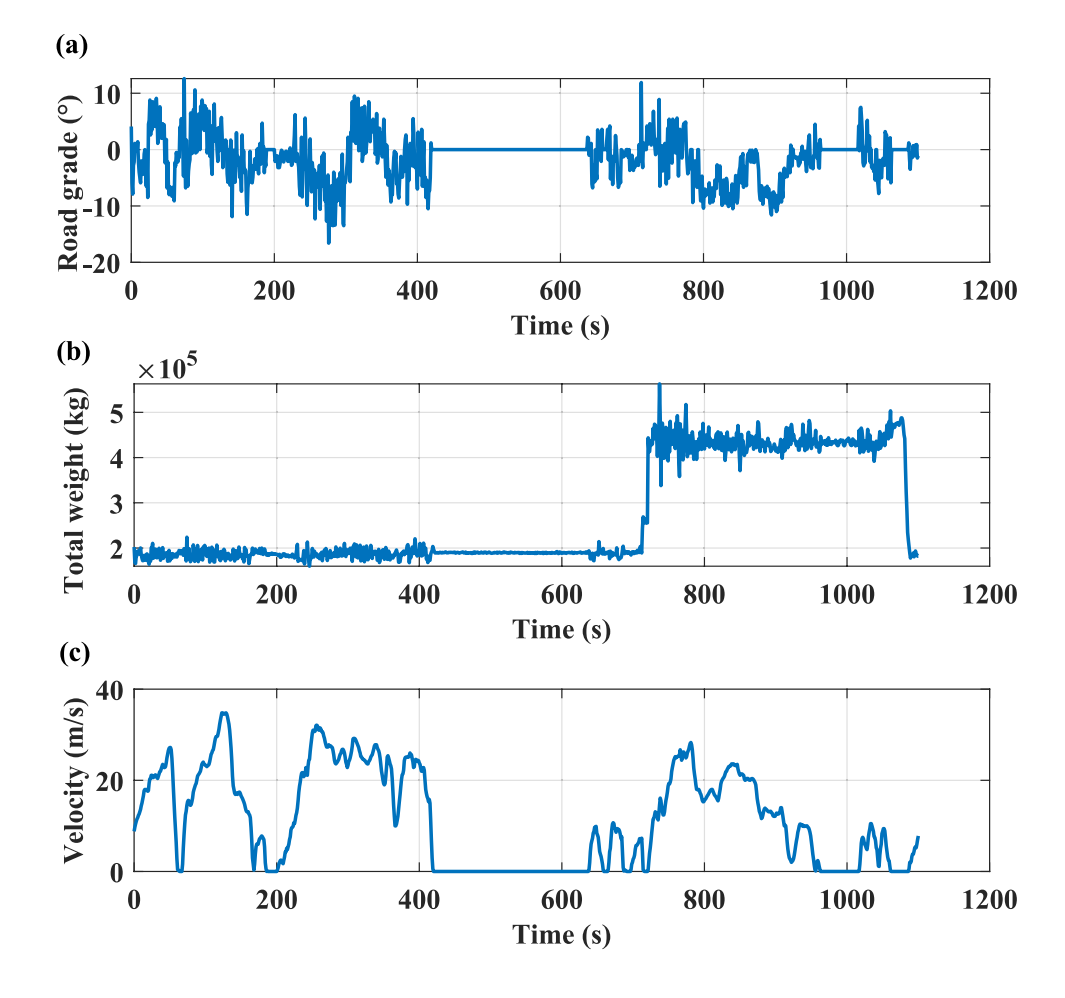
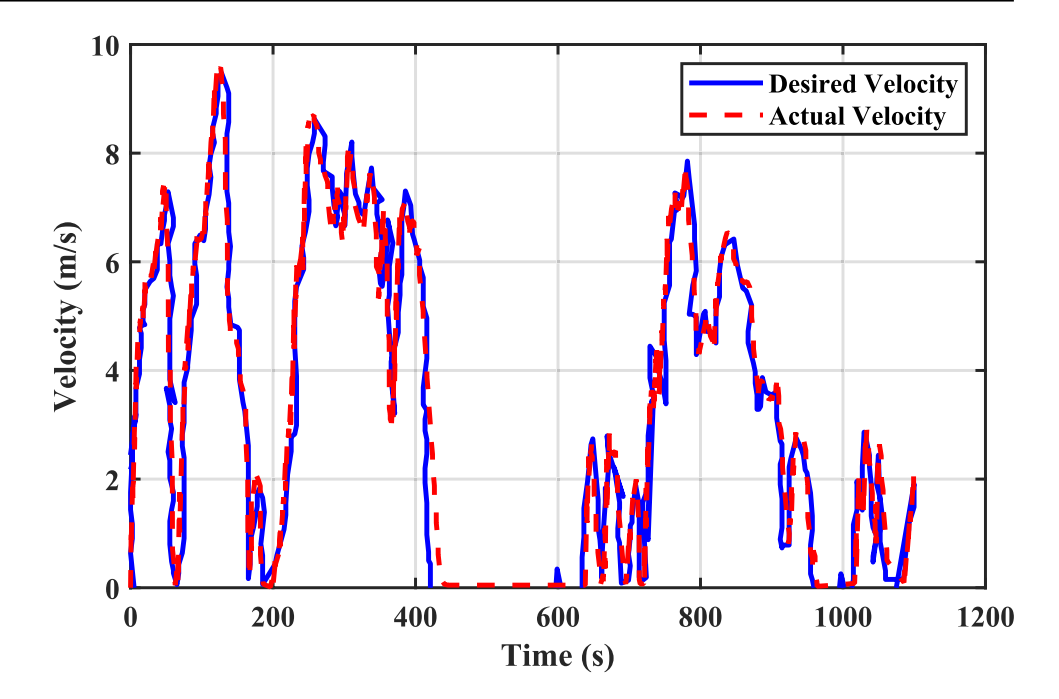




Fig. 9 Simulated velocity compared to the actual (input) velocity of the vehicle



Komatsu 830E-5 truck, with the expectation of providing a maximum power of 1865 kW. Lastly, the propelling force is positive throughout the simulation indicating it overcomes all the resistive forces as one would expect for this duty cycle. The force provides the correct acceleration, which can be verified by the accurate output velocity from the truck model (Fig. 9). Overall, the authors conclude that the model behaves as expected and is suitable for the simulation experiments in this work to provide a basis for the discussion in this paper.

# 3.3 Simulation Experiments

The authors conducted simulation experiments to estimate fuel consumption under different duty cycles using the data acquired from a mine. The haulage cycle data from the mine contains 30 different drive cycles from the same mine. Each drive cycle consists of six different vehicle states: "empty run," which signifies when the truck moves without any loaded ore or waste; "empty stop," which indicates that the truck is not moving and empty; "loading" which is when the truck is without motion but loading materials; "dumping run", which is when the vehicle is offloading the materials; and "hauling stop," which indicates that the vehicle is loaded but without motion. The drive cycle will be simulated with the grades. To reduce computational time from simulating the long waiting times where there is negligible energy consumption (Fig. 9), we modified some drive cycles for simulation (by removing the idle times) to minimize the simulation time and computational expense. However, we kept all the other data the same.

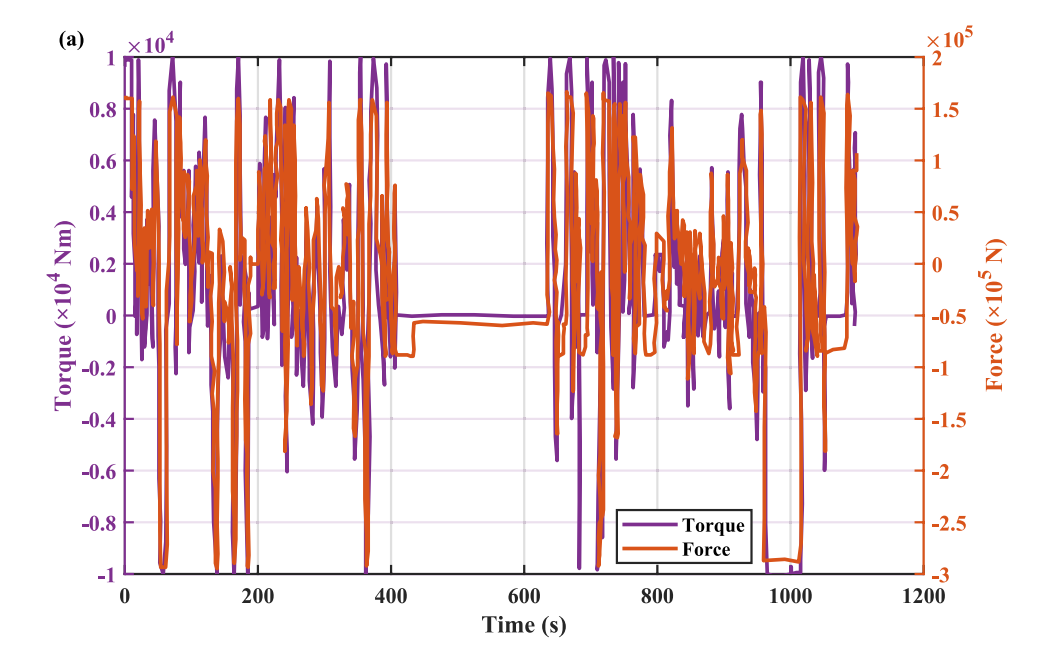
It is important to note that in most scenarios, when trucks are stationary in mine operations, power and fuel consumption may not be zero because other activities, such as raising the bucket or dumping ore in mining equipment, require energy even if there is no motion. In the truck data provided for this model, there is fuel consumption when the trucks are stationary. However, the model in this work only predicts energy and fuel consumption when the truck is in motion, since this model uses propelling speed to trigger power and fuel consumption. While this is a limitation of the work, it is not a significant drawback, as most of the energy and fuel consumption is attributed to truck motion. Although scenarios such as dumping may sometimes yield higher fuel consumption than the average no-motion activities, the difference between the fuel consumption associated with these and the motion activities is still high.

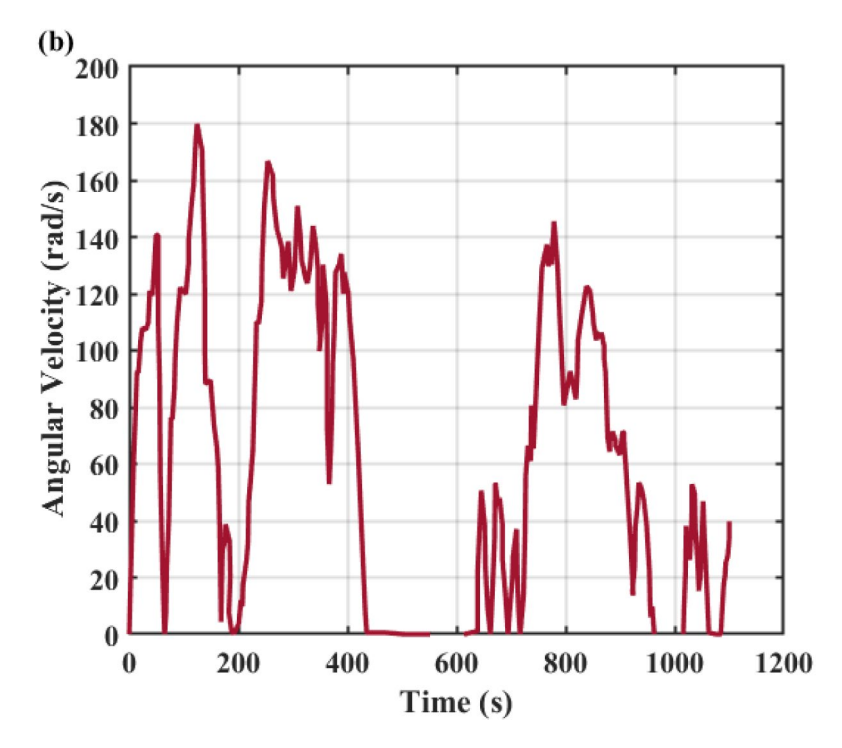
The simulation experiments showcase three different scenarios based on simulations that vary based on cycle time. The first experiment and its associated results are derived from the verification simulation above. It will be regarded as a medium-length scenario based on the simulation time. The second experiment is a shorter simulation (cycle time), while the third experiment is from a longer simulation (cycle time) to evaluate the sensitivity of the fuel consumption to differences in haulage cycle times. This section will compare the sum of both fuels used to understand the difference in the amount of fuel used in both technologies for each of the simulations.

For each drive cycle, the analysis estimated the amount of diesel and hydrogen fuel consumed using the simulation results. The total amount of diesel fuel consumed was



**Fig. 10** Results from simulation for **a** force and torque and **b** angular velocity





derived from the mine data provided by integrating the rate of fuel consumed over the corresponding period (Fig. 13). While for each hydrogen fuel, the total fuel rate comes from the model simulation. The obtained hydrogen fuel rate is integrated over the period of each drive cycle to attain the sum of hydrogen used. For example, the drive cycle utilized for the model verification is used as the result for the medium simulation case.

# 3.3.1 Medium Haul Cycle Case

Figure 14 shows the rate of diesel fuel consumption and the total fuel consumption. For this haul cycle, the truck consumes 29.025 L of diesel over the sampled period. To obtain the amount of hydrogen consumed, the simulation produces two plots: the rate of hydrogen consumed and the sum of hydrogen consumed over time (Fig. 15). Over the sampled period, the truck consumed 24,081 standard liters



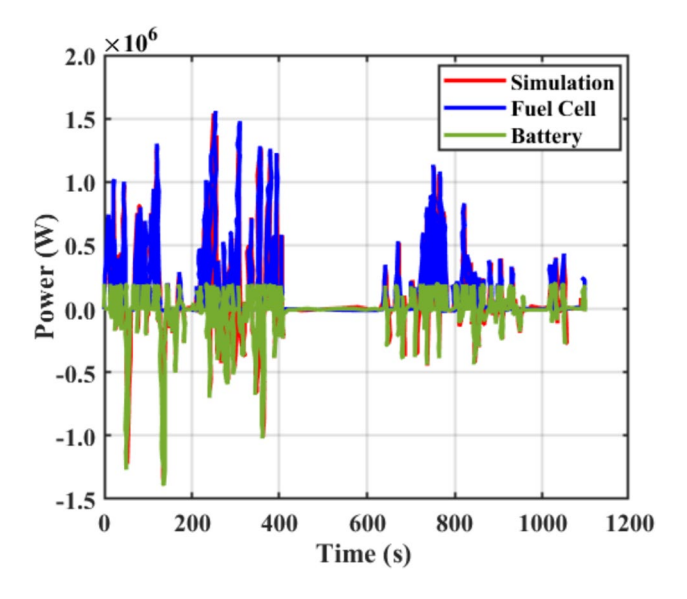


Fig. 11 Power requested from simulation; and predicted power for fuel cell and battery

of hydrogen at standard temperature and pressure (STP)—a pressure of around 1 bar.

# 3.3.2 Short-Haul Cycle Case

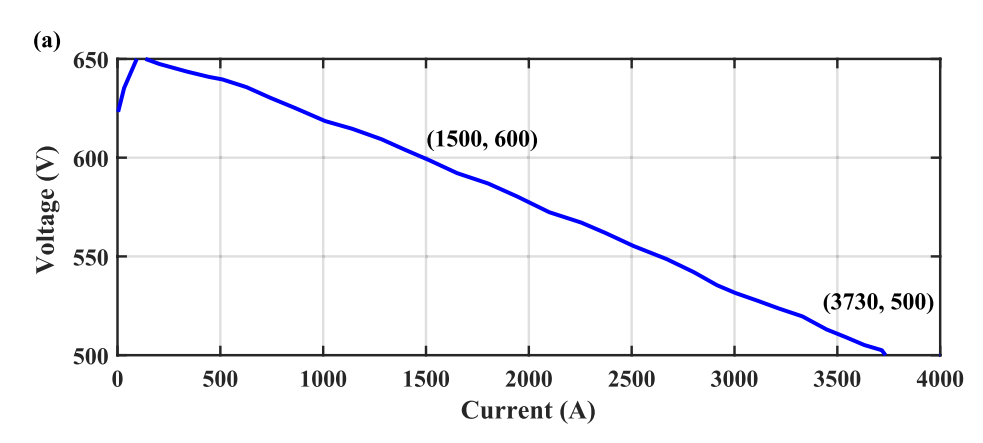
The short simulation case is the shortest simulation with a duration of 852 s (Figure 16a). The model took in the drive cycle, which includes speed, varying grade (inclination), and mass of the truck, shown in Figure 16, respectively. This was a complete drive cycle without any alteration. This scenario helps to show how the model operates in an environment of consistent high-performance operation within a short period of time and the swift change in operating states.

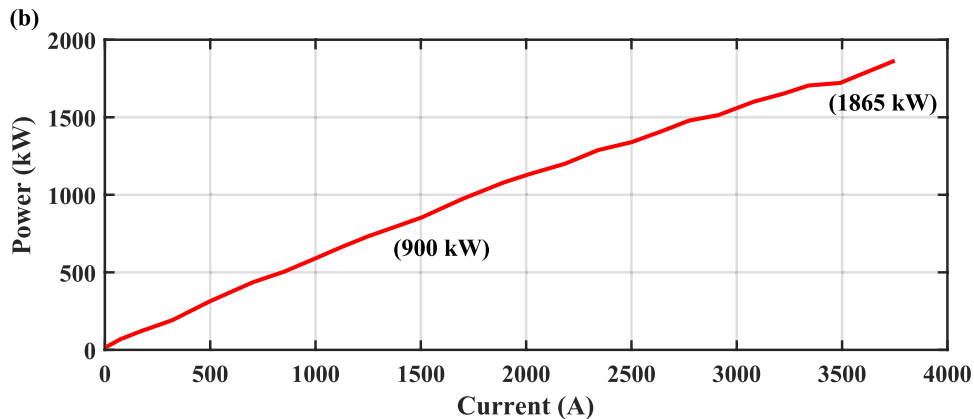
As with the previous example, Fig. 17 shows the rate of and total amount of diesel consumed over the duty cycle, while Fig. 18 shows the same for hydrogen. Figure 17 shows the truck consumed 23.6 L of diesel over the sampled period, and Fig. 18 shows the truck consumed 17,729 L of hydrogen (at STP) over the sampled period.

# 3.3.3 Long-Haul Cycle Case

The third simulation is the longest simulation, with a duration of 1551 s, as seen in Fig. 19. It helps to show how the model operates in an environment of consistent high-performance operation over a long duration. Figures 20 and

**Fig. 12** Voltage-current characteristics of the fuel cell stack







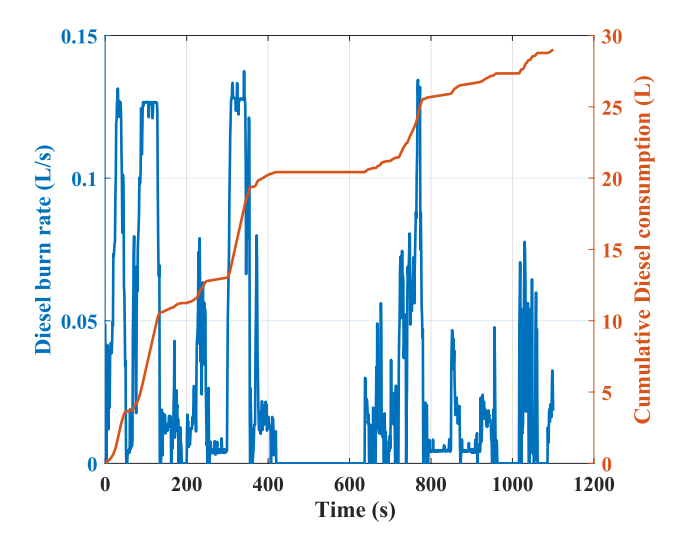


Fig. 13 Diesel fuel rate

21 show the diesel and hydrogen consumption rates, respectively. The results show the trucks consume 82.94 L of diesel and 25,705 L of hydrogen over this duty cycle.

# 3.3.4 Hydrogen Storage and Fuel Cell Volume Estimation

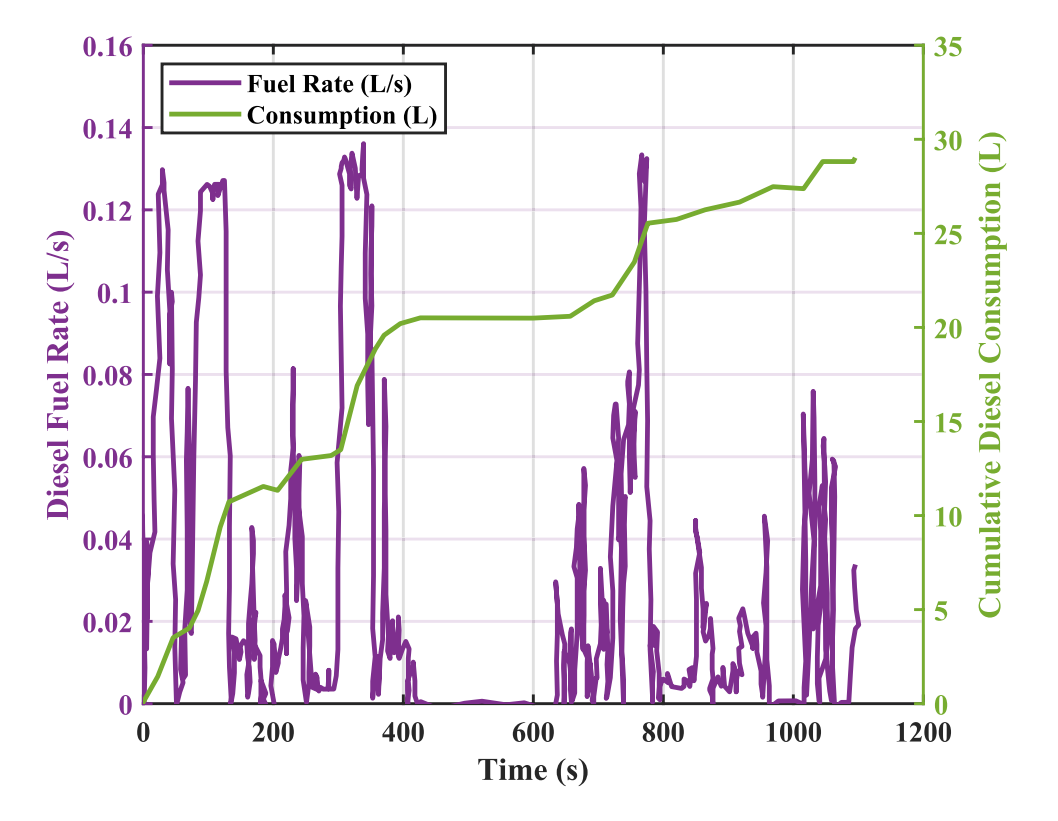
The simulation model estimates the hydrogen fuel consumption at 1 bar. However, the authors estimated the hydrogen volume at 350 bar and 700 bar for each drive cycle because,

as an industry standard, most fuel cell vehicles have hydrogen pressurized to 350 bar or 700 bar. Table 5 shows the results of this analysis for the three drive cycle cases. The higher pressure increases the density of hydrogen and reduces the storage volume requirements significantly. At 1 bar, hydrogen is approximately 0.09 kg/m³ compared to 21 kg/m³ and 42 kg/m³, respectively, at 350 and 700 bars (Table 5).

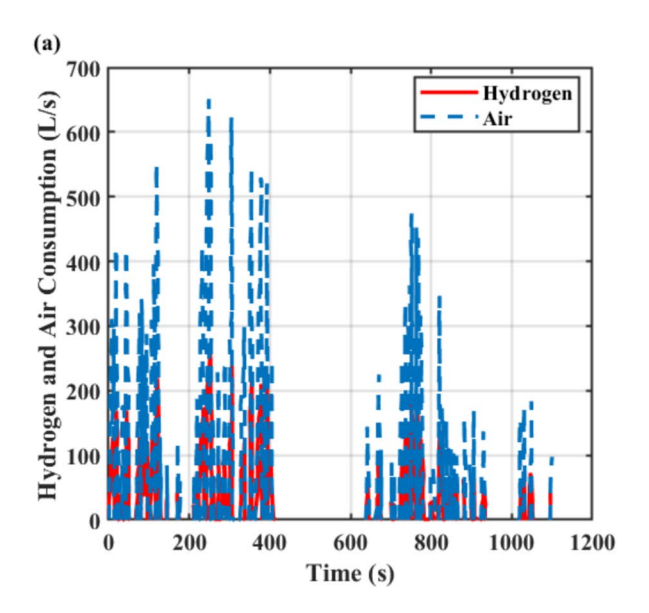
Table 5 shows that, for hydrogen tanks to provide similar range and storage, the hydrogen in mining trucks should be pressurized at 700 bars, as the difference in volume at 350 bars will be too high. Therefore, for the short drive cycle, with a pressure of 700 bars, the volume of hydrogen required to power the drive cycle would be 37.99 L. In general, except for the long drive cycle, the volume of diesel required is lower than the volume of hydrogen required at 700 bars. The fact that the hydrogen fuel cell truck appears to use a lower volume of hydrogen on the long drive cycle shows that the hydrogen fuel efficiency varies according to the duty cycle.

Even then, it is important to note that the required hydrogen tank to provide the 4542 L of storage (the capacity of the Komatsu 830-E truck) [21] will be bulkier than the current diesel tank because of need to pressurize the hydrogen to 700 bars. Also, other factors such as the fuel cell stack size, the capacity of the auxiliary power source, and power distribution strategy between the fuel cell and the other power source play a significant role when designing the fuel cell truck. The prediction of fuel cell stack size is highly

Fig. 14 Diesel fuel rate and sum of diesel consumed over time for medium haul cycle







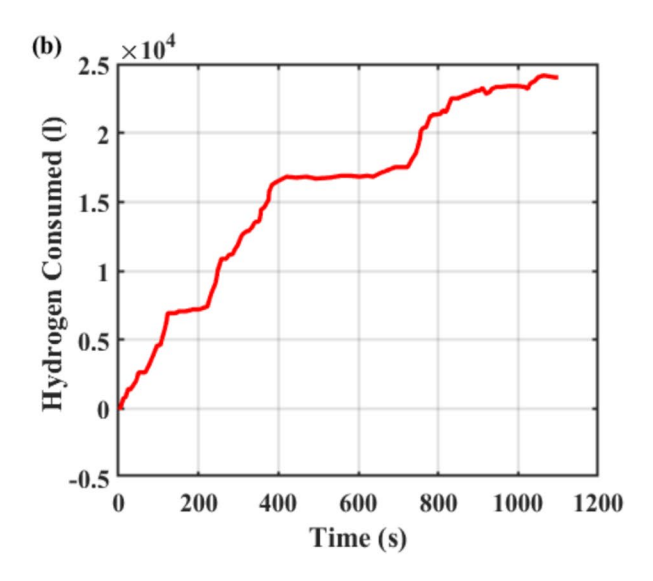


Fig. 15 (a) Hydrogen and Air consumption rate and (b) Sum of Hydrogen consumed over time for medium haul cycle case

dependent on the maximum power and voltage requirements [22]. In this case, the maximum power and voltage requirements are: power of 1865 kW, voltage of 625 V, and current of 2800 A. We used a CAT diesel engine (C175-16) to guide our estimates for the size of the powertrain because we did not have access to the dimensions and specifications of the engine in the Komastu truck. The CAT C175-16 [23] has a similar power rating to the Komatsu truck's engine. The fuel cells, in this work, have an assumed current density of 0.6A/cm<sup>2</sup> [21]. The 2800 A current will equate to 4666A/ cm<sup>2</sup> of the total active cell area and 957 cells in the stack. For a 1865 kW power requirement, the system may need up to  $8.4 \times 10^6$  cm<sup>3</sup> for fuel cell powertrain. Nuvera Fuel Cell produces a 67 kW fuel cell engine with a  $3.0 \times 10^5$  cm<sup>3</sup> volume of space [24]. The  $8.4 \times 10^6$  cm<sup>3</sup> for the fuel cell engine compares to  $28.6 \times 10^6$  cm<sup>3</sup> at the minimum for a diesel engine [21].

#### 3.4 Discussions

Fuel cell electric vehicles powered by hydrogen can have similar performance characteristics to the internal combustion engine, but with no direct GHG emissions [25]. Even though the integration of fuel cells into a truck will reduce GHG emissions in mining, there are many challenges to overcome to make hydrogen-powered fuel cell trucks a reality. This section uses the simulation results and the literature to guide a discussion on the important opportunities and challenges associated with incorporating hydrogen fuel cells in mining trucks. Most of the challenges involve the truck's real estate management during redesigning, the cost of parts and infrastructure, and fuel cell performance. The

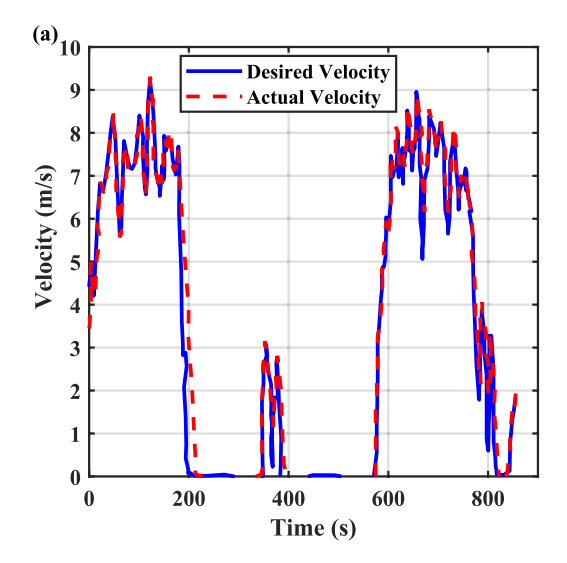
main opportunity is that hydrogen-powered fuel cell trucks can help reduce GHG emission in mining and help mining firms achieve their ESG (environmental, social, and governance) commitments around greenhouse gas emissions.

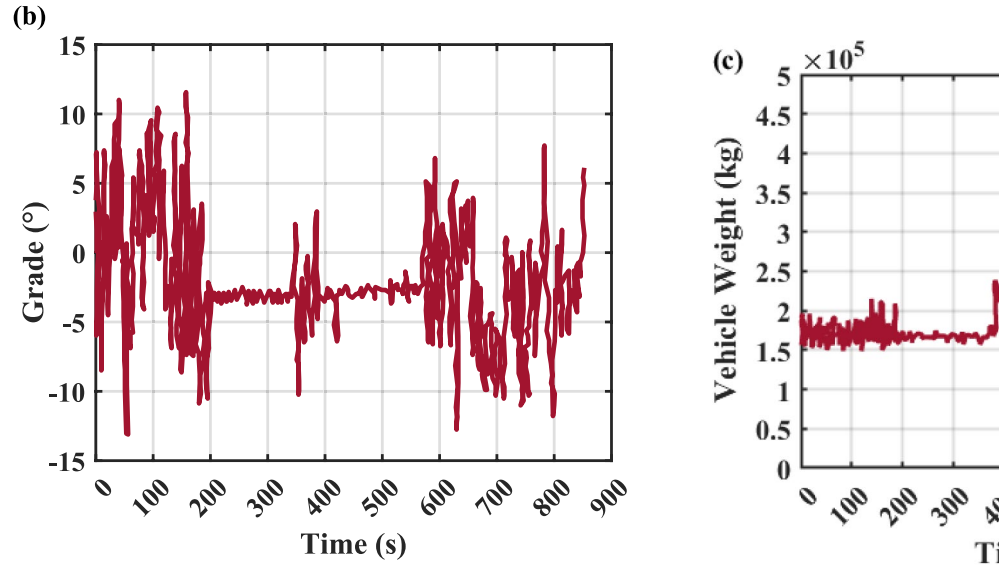
# 3.4.1 Vehicle Real Estate

As illustrated by our simulation results, it is technically possible to power a truck with a hydrogen fuel cell powertrain. However, the challenge is in the feasibility of directly replacing an internal combustion powertrain and fuel storage with a hydrogen fuel cell system engine, which we believe is the quickest pathway to widespread adoption. The simulation results in Sect. 3.1 show that a Komatsu 830E will require 38 to 55 L of hydrogen at 700 bars for the simulated duty cycles. This means the truck may need more space for the hydrogen fuel storage (i.e., even in the long-haul case, because of the additional material required to keep the hydrogen pressurized, the space required for the same amount of driving range is likely to be higher). The higher fuel burn rate will increase the need for refueling, which will reduce production rates. For example, for the medium length duty cycle, the simulation results show that the hydrogenpowered truck can only do 88 such cycles before the tank is empty, compared to 156 cycles for the equivalent dieselpowered truck.

The internal real estate available for the diesel tank and the diesel engine is not enough to fit in the hydrogen storage and fuel cell stack and maintain the same driving range. Additionally, more space is required for additional components such as batteries, electric motors, and inverters [26] to support the hydrogen fuel cell system to achieve the desired







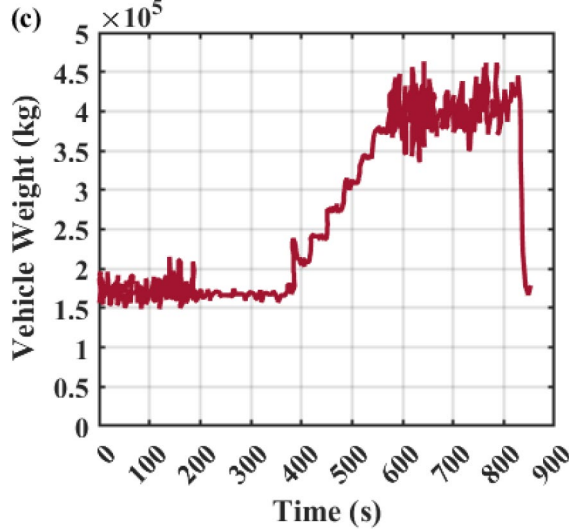


Fig. 16 a Simulated velocity compared to the actual (input) velocity of the vehicle, b grade over time, and c calculated total truck weight over time for short-haul cycle case

output and ensure a safe and efficient system. For example, Anglo American's test truck uses a 1.2 MWh lithium-ion battery pack and multiple fuel cells to deliver up to 800 kW of power [27] for a Komatsu 930E truck (rated capacity of 290 tonnes).

Thus, retrofitting the existing diesel-powered trucks to become hydrogen fuel cell trucks will require more engineering redesign than simply replacing the internal combustion drive train components with fuel cell drive train components. One option, which is not that desirable, is to reduce the carrying capacity of the truck (by reducing the size of the truck bed) to create more room for the fuel cell drive train components. Another alternative is to use newer technologies to store hydrogen at higher pressures and thus decrease the volume requirements. For example, the cryocompression technique, which uses liquid nitrogen to cool the tank, can provide three times the volumetric capacity of a non-cooled hydrogen tank [28]. Another common method of increasing capacity is utilizing mechanical compression at high pressures, such as 350 bar or 700 bar, because it is a reliable, efficient, and simple approach to the design of hydrogen storage tanks [29] [30]. Mechanical compression helps to increase the volumetric and gravimetric capacity of hydrogen. However, the approach poses safety concerns. The system under high pressure can damage the tank walls because of the Joule-Thomson effect that increases the temperature during refueling [31]. Also, storing hydrogen at pressures higher than 700 bars (this is what will reduce the



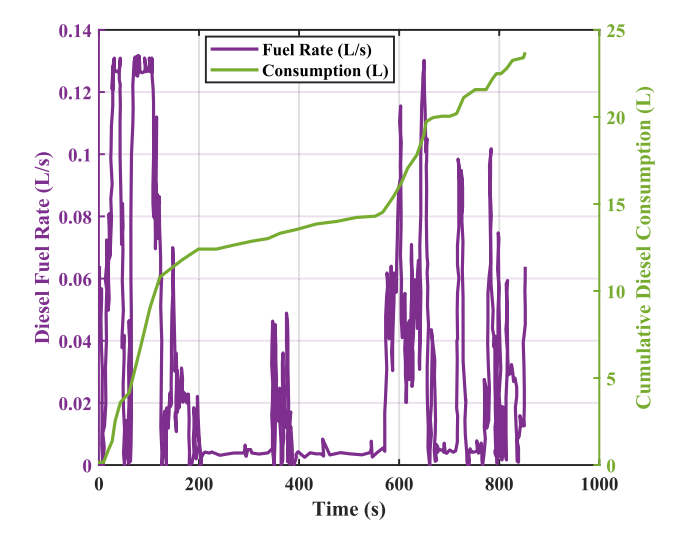


Fig. 17 a Rate of diesel and b sum of diesel consumed over time for short-haul cycle

volume requirements per our simulation results) increases the safety risks.

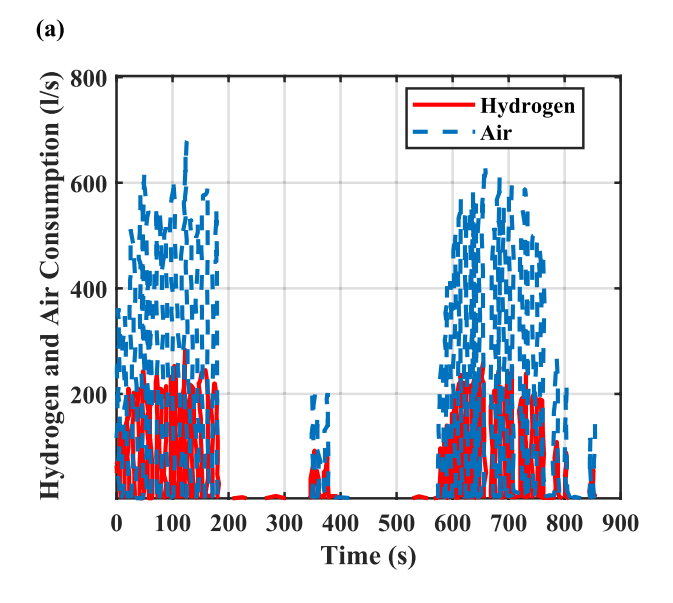
All these challenges may require original equipment manufacturers (OEMs) to design entirely new trucks that are powered by the hydrogen fuel cell power train because the internal real estate of the current diesel-powered trucks may not be enough to fit every component of the fuel cell trucks. OEMs will have to design and manufacture an entirely new truck, which means they have to change their production lines and invest in equipment and materials. Also, this will require that mine operators trust and accept the new products.

#### 3.4.2 Infrastructure and Manufacturing

The process of changing production lines and factories may take time and can be expensive. General Motors is expected to spend about \$7 billion on a single battery plant to support the transition to electric vehicles [32]. For OEMs to make this level of investment, they must be confident that the return on investment is favorable and the associated risks are manageable. Similarly, the materials used in manufacturing components for hydrogen fuel cell systems are currently more expensive than those used in conventional diesel trucks. Due to these higher material costs, hydrogen fuel cell systems and proposed trucks are likely to be significantly more expensive than their diesel counterparts.

A key driver of this cost gap is the absence of economies of scale due to the lack of mass production. Without substantial market demand—such as from mine operators—or supportive government policies and incentives, OEMs are unlikely to commit the required capital. While some diesel-powered electric drive trucks may already contain components compatible with fuel cell systems, the additional space needed for hydrogen storage and thermal management systems may still necessitate the development of an entirely new vehicle platform, thus preserving the need for substantial investment.

Beyond the OEM investments, successful integration of hydrogen fuel cells into the mining industry also requires mine operators to invest in hydrogen production and distribution infrastructure. Hydrogen production costs remain a major hurdle, especially for low-emission pathways. Cleaner hydrogen production methods, such as electrolysis and steam methane reforming with carbon capture, are significantly



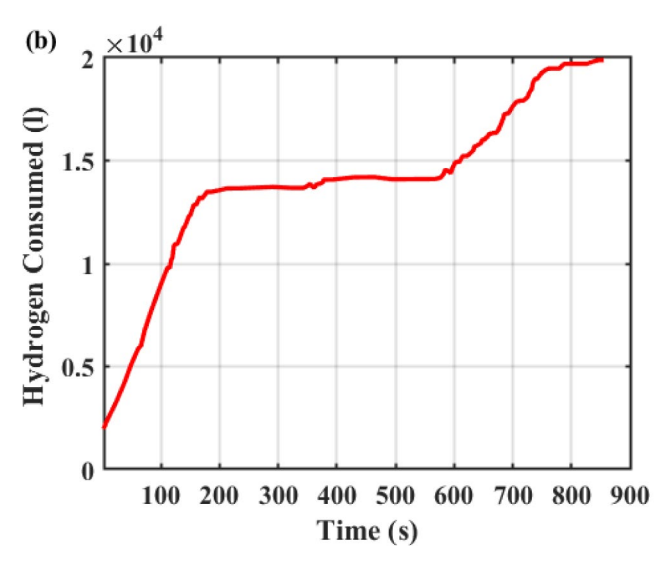


Fig. 18 a Hydrogen and air consumption rate and b sum of hydrogen consumed over time for short-haul cycle



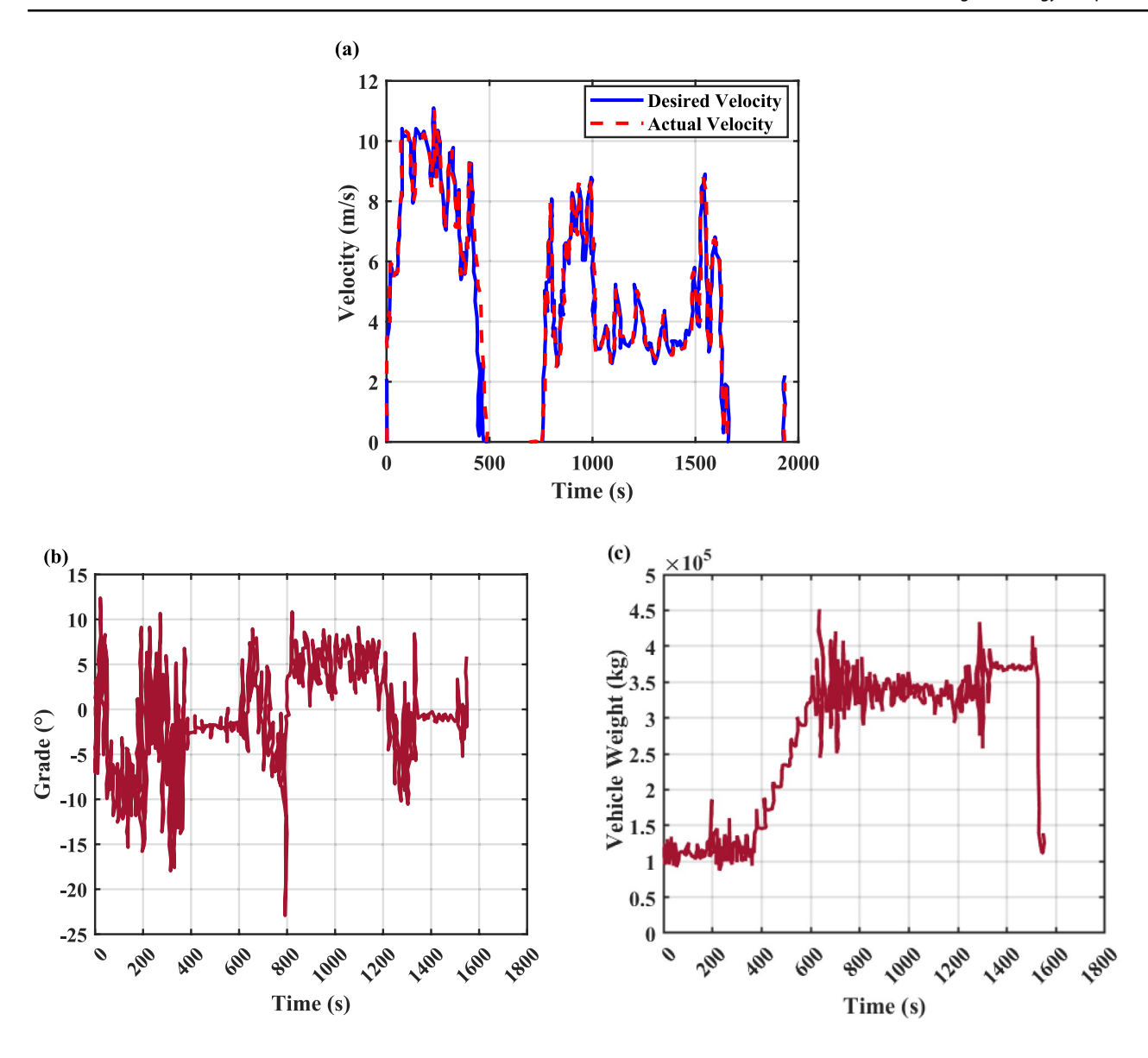


Fig. 19 a Simulated velocity compared to the actual (input) velocity of the vehicle, b grade over time, and c calculated total truck weight over time for long-haul cycle case.

more expensive—two to three times the cost of hydrogen produced from conventional natural gas sources [33]. Additionally, hydrogen distribution to mines will require a new logistical platform. While blending hydrogen with natural gas in existing pipelines has been proposed [34], this method falls short of achieving zero greenhouse gas emissions, thereby limiting its suitability for long-term decarbonization goals.

Security concerns also pose a critical barrier to the widespread deployment of hydrogen systems in mining environments. Due to the need for large-scale on-site hydrogen generation and storage, mines may have to manage significant volumes of highly flammable gas in proximity to other hazardous materials, including explosives commonly used in mining operations. This raises substantial safety and security risks, including vulnerability to accidental ignition, sabotage, or targeted attacks. As such, rigorous safety protocols and secure infrastructure will be essential to mitigate these risks and gain stakeholder and regulatory approval for hydrogen deployment in mining applications.

# 3.5 Conclusions

Hydrogen fuel cell technology presents a viable pathway toward decarbonizing heavy-duty mining haul trucks, offering a cleaner alternative to diesel engines. This work applied vehicle drive train and energy simulation in MAT-LAB/Simulink to inform a discussion of the challenges and



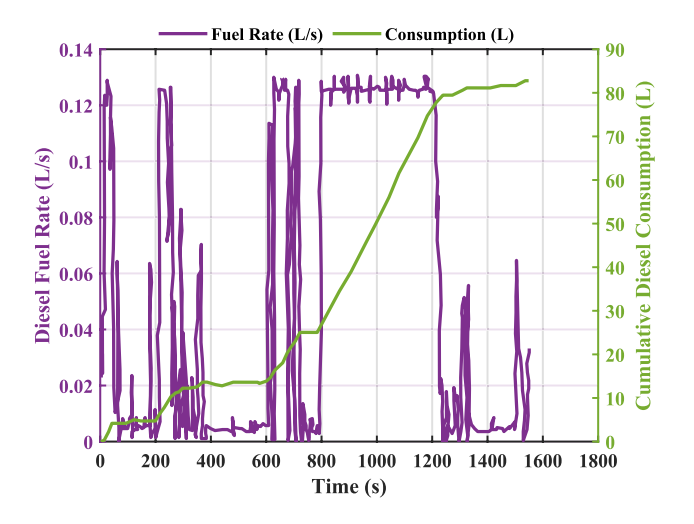
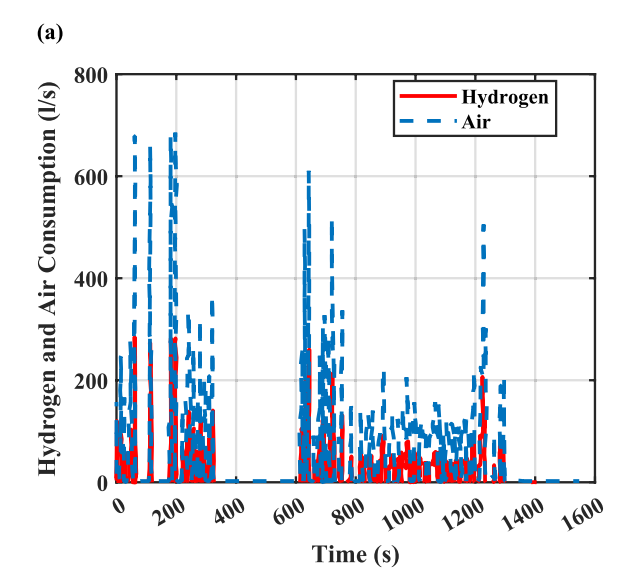


Fig. 20  $\, a$  Rate of diesel and  $\, b$  sum of diesel consumed over time for long-haul cycle.

opportunities of incorporating hydrogen fuel cell drive trains into the current form factors of mine haul trucks. Using a validated MATLAB/Simulink model based on the Komatsu

830-E truck, this study estimated the hydrogen requirements for short-haul, medium-haul, and long-haul cycles and evaluated fuel cell stack sizing based on power, voltage, and current demands. The results show that the short-, medium-, and long-haul duty cycles require 75.98, 103.19, and 110.16 L of hydrogen, respectively, at 350 bars, and 37.99, 51.40, and 55.08 L, respectively, at 700 bars. This compares to 23.60, 29.03, and 82.92 L of diesel, respectively, for short-, medium-, and long-haul duty cycles. These results show that the most likely pressure to store hydrogen on a mining truck (to maintain driving range and similar real estate) is 700 bars. Even at 700 bars, the truck real estate is not enough to provide space for adequate hydrogen storage, fuel cell stack, and other components of the fuel cell drive train (including battery pack) to allow for retrofitting current diesel truck models as hydrogen fuel cell trucks. Thus, the most likely path to hydrogen fuel cell trucks will involve a more extensive redesign that will require significant investment from original equipment manufacturers. Additionally, mining companies that adopt hydrogen fuel cell trucks have to be willing to invest in hydrogen storage and transportation infrastructure and address safety and security risks.



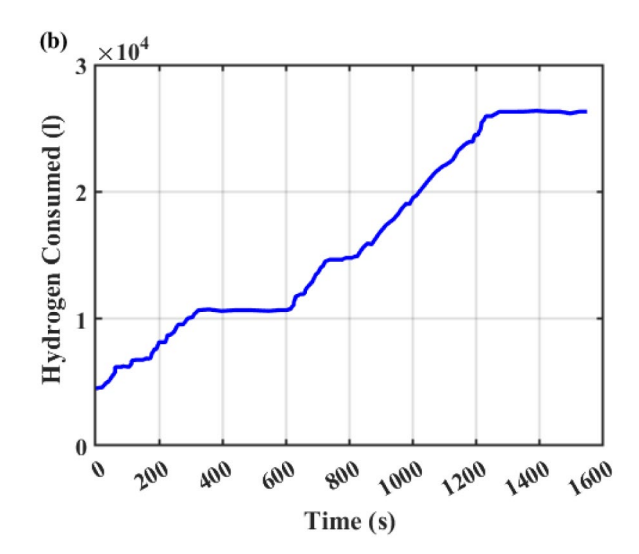


Fig. 21 a Hydrogen and air consumption rate and b sum of hydrogen consumed over time for long-haul cycle.

**Table 5** Showing the volume of hydrogen by pressure for all drive cycles

Hydrogen pressure and density		Drive cycle: base case	Drive cycle: short	Drive cycle: long
		Diesel fuel consumed: 29.025 L	Diesel fuel consumed: 23.6 L	Diesel fuel consumed: 82.923 L
Pressure (bar)	Density (kg/m <sup>3</sup> )	Volume (L)	Volume (L)	Volume (L)
1	0.09	24,081	17,729	25,705
350	21	103.19	75.98	110.16
700	42	51.4	37.99	55.08



Future work is necessary to extend the model by incorporating real-world operating conditions—such as variable power demands, temperature effects, and system degradation—to better predict long-term performance and durability of fuel cell systems. Overall, this work outlines both the technical feasibility and the systemic challenges associated with transitioning to hydrogen fuel cell technology in mining haulage, providing a foundation for future design and deployment strategies.

**Author Contribution** Dr. Kwame Awuah-Offei is a member of the MME Editorial Board. He will not be involved in the review of this manuscript.

**Funding** This research was funded by the Union Pacific/Rock Mountain Energy Foundation Professorship in Mining Engineering. The endowment and the original donors do not have any direct interest in the outcomes of this research.

Union Pacific/Rocky Mountain Energy Profersorship

**Data Availability** The data that support the findings of this study are available from the corresponding author upon reasonable request. Due to the need for additional context regarding the interpretation and appropriate use of the data, interested researchers are encouraged to contact the corresponding author via email to obtain access.

Open Access This article is licensed under a Creative Commons Attribution 4.0 International License, which permits use, sharing, adaptation, distribution and reproduction in any medium or format, as long as you give appropriate credit to the original author(s) and the source, provide a link to the Creative Commons licence, and indicate if changes were made. The images or other third party material in this article are included in the article's Creative Commons licence, unless indicated otherwise in a credit line to the material. If material is not included in the article's Creative Commons licence and your intended use is not permitted by statutory regulation or exceeds the permitted use, you will need to obtain permission directly from the copyright holder. To view a copy of this licence, visit http://creativecommons.org/licenses/by/4.0/.

#### References

- Delevingne L, Glazener W, Grégoir L, Henderson K (2021) Climate risk and decarbonization: what every mining CEO needs to know. McKinsey & Company. Available at: https://www.mckinsey.com/capabilities/sustainability/our-insights/climate-risk-and-decarbonization-what-every-mining-ceo-needs-to-know#/. Accessed 12 May 2025
- ICMM (International Council on Mining and Metals) (2021)
   Position statement: Climate change. London, United Kingdom.
   Available at: https://www.icmm.com/en-gb/our-principles/posit ion-statements/climate-change. Accessed 9 June 2025
- Aramendia E, Brockway PE, Taylor PG, Norman J (2023) Global energy consumption of the mineral mining industry: exploring the historical perspective and future pathways to 2060. Glob Environ Change. https://doi.org/10.1016/j.gloenvcha.2023.102745
- Muralidharan R, Kirk T, and Koch Blank T (n.d.) Pulling the weight of heavy truck decarbonization. Exploring pathways to decarbonize bulk material hauling in mining. Available at: https:// rmi.org/wp-content/uploads/2019/06/rmi-pulling-the-weight-ofheavy-truck-decarbonization.pdf. Accessed 24 June 2025

- Weiss H, Winkler T, Ziegerhofer H (2018) Large lithium-ion battery-powered electric vehicles—from idea to reality. In: 2018 ELEKTRO. pp 1-5. Available at: https://ieeexplore.ieee. org/stamp/stamp.jsp?tp=&arnumber=8398241Joule4:511-515. Accessed 12 May 2025
- McGinnis R (2020) CO2-to-fuels renewable gasoline and jet fuel can soon be price competitive with fossil fuels. Joule 4(3):509– 511. https://doi.org/10.1016/j.joule.2020.01.002
- Valenzuela M, Cruzat J (2018) Modeling and evaluation of benefits of trolley assist system for mining trucks. IEEE Trans Ind Appl pp 1. https://doi.org/10.1109/TIA.2018.2823261
- Venditti B (2025) Charted: Coal still dominates global electricity generation. Energy Shift. Available at: https://elements.visualcapi talist.com/charted-coal-still-dominates-global-electricity-gener ation/. Accessed 23 June 2025
- APPIAN INSIGHTS (2022) Mining and the energy link: synergies, challenges, and opportunities. Available at: https://appiancapitaladvisory.com/insights-mining-and-the-energy-link-synergies-challenges-and-opportunities/#:~:text=Therefore%2C%20it%20is%20no%20surprise,of%20the%20renewable%20energy%20generation. Accessed 23 June 2025
- Veziroglu A, MacArio R (2011) Fuel cell vehicles: state of the art with economic and environmental concerns. Int J Hydrogen Energy 36(1):25–43. https://doi.org/10.1016/j.ijhydene.2010.08. 145
- Emadi, A., Williamson, S. S. (2004) Fuel cell vehicles: opportunities and challenges. In *IEEE Power Engineering Society General Meeting 2004*. (pp 1640–1645). Available at: https://ieeexplore.ieee.org/stamp/stamp.jsp?tp=&arnumber=1373150&tag=1. Accessed 12 May 2025
- Toyota (2022) 2023 Toyota Mirai. Available at https://www.toyota.com/mirai/. Accessed 12 May 2025
- Hyundai (2022) XCIENT fuel cell Hyundai. Available at: https:// trucknbus.hyundai.com/global/en/products/truck/xcient-fuelcell. Accessed 12 May 2025
- Anglo American Platinum Limited (2022) Interim results 2022. London, United Kingdom. Available at: https://www.valterraplatinum.com/~/media/Files/A/Anglo-American-Group/Platinum/report-archive/2022/integrated-annual-report-2022.pdf. Accessed 12 May 2025
- Komatsu America Corp (2019) Komatsu 830E-5 brochure. pp 1–20. Available at: https://www.smsequipment.com/getmedia/ c0aac900-44bb-49ca-bdbc-d1ceaf37604e/830E-5.pdf. Accessed 12 May 2025
- Aström KJ, Murray RM (2010) Feedback systems: an introduction for scientists and engineers. Princeton University Press, Available at: (https://www.cds.caltech.edu/~murray/books/AM08/pdf/am08-complete\_28Sep12.pdf)
- Ho AK (2020) Fundamentals of PID control pp 1–10. Available at: https://pdhonline.com/courses/e331/e331content.pdf. Accessed 12 May 2025
- Inoue K, Ogata K, Kato T (2007) A study on an optimal torque for power regeneration of an induction motor II. Design methodology of regenerative torque A. Objective system. Available at: https://ieeexplore.ieee.org/stamp/stamp.jsp?tp=&arnumber= 4342332. Accessed 12 May 2025
- Jethani P (2017) Power management strategy of a fuel cell hybrid electric vehicle with integrated ultra-capacitor with driving pattern recognition. Thesis (Master of Science), Arizona State University. Available at: https://shorturl.at/EiHxL
- Adegbohun F, von Jouanne A, Phillips B, Agamloh E, Yokochi A (2021) High performance electric vehicle powertrain modeling, simulation and validation. Energies. https://doi.org/10.3390/en140 51493
- 21. Akinrinlola A (2022) Replacing combustion engines with hydrogen fuel cells to power Replacing combustion engines with



- hydrogen fuel cells to power mining haul trucks: challenges and opportunities mining haul trucks: challenges and opportunities. Thesis (Master of Science), Missouri University of Science and Technology, United States. Available at: https://scholarsmine.mst.edu/cgi/viewcontent.cgi?article=9107&context=masters\_theses. Accessed 27 Aug 2025
- Spiegel C (2007) Designing and building fuel cells, 1st edn. McGraw-Hill Professional, New York
- CATERPILLAR. Product specifications for C175–16 diesel generator sets. Available at: https://www.cat.com/en\_US/products/new/power-systems/electric-power/diesel-generator-sets/10000 28916.html. Accessed 27 Aug 2025
- Nuvera fuel cells (n.d.) Engines redefined. Available at: https:// www.nuvera.com/enginesredefined. Accessed 24 June 2025
- Stoddard E (2022) A hydrogen monster truck at an Anglo American Platinum mine heralds a future with zero emissions. Daily Maverick. Available at: https://www.dailymaverick.co.za/article/2022-05-08-a-hydrogen-monster-truck-at-an-anglo-american-platinum-mine-heralds-a-future-with-zero-emissions/. Accessed 24 June 2025
- Yue M, Lambert H, Pahon E, Roche R, Jemei S, Hissel D (2021) Hydrogen energy systems: a critical review of technologies, applications, trends and challenges. Renew Sustain Energy Rev. https://doi.org/10.1016/j.rser.2021.111180
- Randall C (2022) Anglo American presents fuel cell heavy-duty mining truck. Electrive.com. Available at: https://www.electrive. com/2022/05/09/anglo-american-presents-fuel-cell-heavy-dutymining-truck. Accessed 24 June 2025
- Durbin DJ, Malardier-Jugroot C (2013) Review of hydrogen storage techniques for on board vehicle applications. Int J Hydrogen Energy 38(34):14595–14617. https://doi.org/10.1016/j.ijhydene. 2013.07.058

- Li M, Bai Y, Zhang C, Song Y, Jiang S, Grouset D, Zhang M (2019) Review on the research of hydrogen storage system fast refueling in fuel cell vehicle. Int J Hydrogen Energy 44(21):10677–10693. https://doi.org/10.1016/j.ijhydene.2019.02.208
- Andersson J, Grönkvist S (2019) Large-scale storage of hydrogen. Int J Hydrogen Energy 44(23):11901–11919. https://doi.org/10. 1016/j.ijhydene.2019.03.063
- Zhang M, Lv H, Kang H, Zhou W, Zhang C (2019) A literature review of failure prediction and analysis methods for composite high-pressure hydrogen storage tanks. Int J Hydrogen Energy 44(47):25777–25799. https://doi.org/10.1016/j.ijhydene.2019.08. 001
- Boudette NE (2022) General Motors to spend \$7 billion on electric vehicle plants. The New York Times. Available at: https://www.nytimes.com/2022/01/25/business/general-motors-electric-vehicle-plant.html. Accessed 24 June 2025
- Bartels JR, Pate MB, Olson NK (2010) An economic survey of hydrogen production from conventional and alternative energy sources. Int J Hydrogen Energy 35(16):8371–8384. https://doi. org/10.1016/j.ijhydene.2010.04.035
- Haeseldonckx D, D'haeseleer W (2007) The use of the naturalgas pipeline infrastructure for hydrogen transport in a changing market structure. Int J Hydr Energy 32(10–11):1381–1386. https:// doi.org/10.1016/j.ijhydene.2006.10.01

**Publisher's Note** Springer Nature remains neutral with regard to jurisdictional claims in published maps and institutional affiliations.

